An Investigation of Diesel-Generator Shaft and Bearing Failures.

by

I.A. Craighead* & T.G.F. Gray

Department of Mechanical Engineering
University of Strathclyde,
Glasgow, G1 1XJ, U.K.
(* Corresponding author: email icraighead@mecheng.strath.ac.uk, tel. (44) 0141 5482840; fax. (44) 0141 5525105)

Abstract: A shaft failure in a 634 kW diesel generator after 4000 hours of operation required investigation, especially when similar sets began to show signs of excessive bearing housing wear. The failure was found to be due to torsional fatigue caused by operation at an unforeseen resonant condition. The damage to the bearing housing of this type of set was also attributed to this behaviour.

Replacement of the bearings and housings and redesign of the flexible coupling has been undertaken to prevent further failures. Modifications to design procedures are now being adopted to ensure similar problems do not occur in other existing or new machines.

Notation.

a - Crack dimension (m)

F – Force (N)

J – Polar moment of area (m^4)

k – Stiffness (N/m)

m – Mass (kg)

P – Power (watts)

r – radius (m)

R- Stress range

θ - Angular displacement (rad)

τ - Shear stress (N/m^2)

ΔK – Stress intensity threshold (N/m$^{3/2}$)

ω – Rotational speed (rad/s)

1. Introduction.

Diesel generator sets are commonly used to provide power for a wide range of applications. Sets can range in size from a few kilowatts to several Megawatts. The medium and large sets are usually powered by a V12 diesel engine driving an a.c. generator through a flexible coupling. The generator is often a four pole machine allowing generation of a.c. power at either 50 Hz or 60 Hz by operating at 1500 rpm or 1800 rpm respectively.

An unexpected shaft failure in a 634 kW set after only 4000 hours of operation (from new) caused concern. This machine was being used to provide 50 Hz power for refrigeration purposes on a ship which operated between Australia and far eastern ports. This concern was heightened when, during the initial stages of the investigation, reports were received that similar sets were showing severe wear of the bearing housing near to the location of the break in the shaft of the original machine. An inspection of the same bearing and housing on the failed machine showed the same pattern of wear, suggesting that a number of machines could potentially fail in this catastrophic manner. The investigation that was undertaken to identify the cause of the failure and the remedies that were employed are described.

2. Shaft Failure Assessment.

The generator shaft that failed was 110 mm diameter at the section where the break occurred. The fracture occurred near to the coupling end of the machine and the fracture surface included the keyway that was used to locate the coupling half on the generator shaft. Figure 1 shows the "generator side" of the failed shaft. The fractured surface was predominantly at 45$^{\text{o}}$ to the shaft axis and showed the classic signs of being a torsional fatigue failure.

The fracture surfaces had suffered significant consequential damage during the failure process so the site of initiation of the fatigue could not be determined with certainty using fractographic methods. Two potential sites were identified; 1) the keyway root 2) a possible indication of a 6 mm material defect, near to the surface of the plain shaft and approximately 20 mm from the keyway.

The shaft material was identified as BS 970 – 080M40 which has a UTS of 600 MN/m^2 and a yield strength of 260 – 300 MN/m^2. ESDU data Item 88008(1) suggests a plain fatigue endurance limit shear strength of 200 MN/m^2 in torsion. The steady state torsional stress in a plain shaft of 110 mm diameter subject to full load is given by:-

$$\tau = P.r/(J.\omega)$$

$$= 634000 \text{ x } 0.055/(1.44 \text{x} 10^{-5} \text{ x } 157)$$

$$= 15 \text{ MN/m}^2$$

It was therefore evident that some form of stress raiser was required and/or some form of dynamic magnification before fatigue failure would occur.

ESDU 86028 (2) provides information on stress concentration factors in standard keyways suggesting that the critical area is at the root where the parallel section meets the semicircular end and stress concentration levels of 3.4 – 4.0 are applicable based on the maximum shear stress in a plain shaft. The keyway root radii were checked to ensure that there was no possibility that they were sharper than the standard forms for which the data was applicable. The keyway dimensions were found to conform to the standard dimensions. This suggested that a fluctuating torsional shear stress of the order of 50 MN/m^2 would be necessary to initiate a fatigue failure from this site. It can be seen from Figure 1 that the fracture surface did include this most highly stressed region of the keyway.

The significance of the suspected 6 mm crack was assessed via a fracture mechanics approach. ESDU 81012 (3) lists fatigue cracking threshold stress intensity values (ΔK_{th}) for a variety of steels. Although the particular steel was not included in (3) a similar steel (0.55% carbon/manganese steel) suggested a ΔK_{th} of 12 MN/m$^{3/2}$ for R = 0.08 reducing to 3.8 MN/m$^{3/2}$ for R = 0.71. Assuming that the principal tensile stress in the plain shaft surface is numerically equal to the nominal torsional shear stress and the crack is orientated at 45° to the shaft axis, the Mode I stress intensity for a 6 mm deep crack is given by:

$$\Delta K_{th} \; = \; \Delta\tau\sqrt{\pi a}$$

where ΔK_{th} could have a value between 3.8 and 12 MN/m$^{3/2}$ and a = 6 mm suggesting crack growth for plain torsional shear stress levels greater than 27 to 87 MN/m^{2}.

Although the precise location of the fatigue crack initiation could not be determined, the analysis showed that either location was possible provided fluctuating shear stress levels in the region of 50 MN/m^{2} were established in the shaft.

3. Bearing Housing Failure.

Whilst the above analysis was being undertaken it was reported that damaged bearings and housings were being found on similar sets, operating under similar conditions. The bearings showing the damage were from the coupling end of the generator, which was adjacent to the site of fracture of the shaft on the original machine, prompting fears that whatever mechanism caused the shaft failure was also acting in these other machines. The coupling end bearing and housing from the failed machine was obtained and investigated.

The bearing was a deep groove radial ball bearing of 120 mm inside diameter. The bearing itself had not failed but the cast iron housing showed excessive wear in the region where the outer race of the bearing sat. Micrometer measurements of the wear indicated reasonably uniform radial wear of 0.21 mm (0.008 inches) suggesting that

the outer race had been rotating within the bearing housing. This hypothesis was supported by circumferential marks and gouges on the outer race and discoloration of the bearing due to heat. Figure 2 shows the outer race of the bearing and the housing showing the wear and the marks. The discoloration showed a bluish tint over a 45° segment suggesting that a temperature of 290^oC had been reached. The centre of this area was blackened so this temperature was considered to be an underestimate of the peak temperature actually attained within the bearing.

The bearing housing also showed signs of melting, plastic deformation and cracks on the inner bore (Figure 2) but this was attributed to the shaft failure rather than action within the bearing prior to the shaft failing.

4. Coupling Investigation.

The coupling consisted of 12 rubber cylinders interspersed between driving and driven steel plates as shown in Figure 3. A visual inspection of the coupling found evidence of mechanical damage to the hub in the form of deformation and burring of some of the drive blades and blade cutting damage in the 6 rubber drive elements. The 6 drive elements had suffered excessive permanent set and all of the elements showed signs of hardening. The increase in hardness suggested that the elements had been subjected to high temperatures. This could have been due to high ambient operating conditions (operating temperatures of 70^oC were common within sets operating in this region) or heat generated within the rubber if it was subjected to excessive, fluctuating compressive loading produced by torsional oscillation of the shafting system.

5. Torsional Damper Investigation.

The torsional damper was an 18 inch viscous damper. A detailed examination was carried out which revealed that there was no damage to the unit and no leaks. The silicone fluid viscosity was measured to be 103,917 c/s compared to the original specification of 100,000 c/s ± 5%. The Teflon bearings of the unit were found to be in

good condition although there was evidence of uneven wear on the thrust bearings suggesting that there had been higher than usual axial loading present. The general conclusion was that the damper had been functioning normally and was not the cause of the failure.

6. System Dynamic Analysis.

The system comprised a V12 diesel engine driving the generator through a flexible coupling. A schematic drawing of the system is shown in Figure 4. At the design stage, the system had been checked for torsional natural frequencies and its response to dynamic forcing from the engine under normal running and misfire conditions. The checks were carried out for full load and 25% load conditions. Table 1 shows a Holzer(4) analysis for the set at full load showing the first torsional natural frequency to be 40.8 Hz. At lower levels of power generation, due to the non-linear nature of the elastomeric components in the coupling, the stiffness of the coupling reduces and at 25% load the 1st torsional natural frequency reduces to 19 Hz.

For a conventional V12 engine with a firing order of 1R,6L,5R,2L,3R,4L,6R,1L,2R,5L,4R,3L, there is a significant torsional excitation at 1 ½ times the shaft rotational frequency (6). When operating at 1500 rpm the 1 ½ order produces an excitation torque at 37.5 Hz. This excitation frequency was therefore at 92% of the first natural frequency when operating at full load. Depending on the amount of damping in the system, operation at this near resonant condition could result in high levels of torsional vibration. However, a forced response analysis had been undertaken by the original designers which showed that dynamic torsional stresses were below 12 MN/m^2 and the dynamic behaviour was considered acceptable. At 25% load, with the 1st natural frequency being much lower, there was little risk of resonance occurring from the 1 ½ order excitation and a forced response analysis indicated no problems.

However, it was considered that at some part load condition there was likely to be a point when the 1st torsional natural frequency would coincide with the 1 ½ times excitation frequency (37.5 Hz) and resonance would occur. Assuming a linear reduction in coupling torsional stiffness with load indicates that this would be achieved when operating at approximately 89% of full load. Table 2 shows the Holzer analysis for this case.

Upon consultation with the operators of the machines it was confirmed that the generators were being routinely operated at part load, especially 80-90% part load.

7. Bearing/Housing Damage.

Even though the probability of torsional resonant operation had been established there was no obvious connection between this and the damage to the bearings and housings which required a rotational, radial force of high magnitude. A forcing mechanism could be envisaged by considering a simplified dynamic equivalent form of coupling (Figure 5). k_1 is an equivalent spring representing half of the rubber elements on one side of a given diameter and k_2 represents the remaining half on the other side of the diameter. Due to manufacturing tolerances, variations in material properties etc. it is unlikely that k_1 will be exactly the same as k_2. Assuming that for the "worst" diameter $k_1 = 0.9.k_2$. The torsional stiffness of the coupling at full load was specified as:-

$$0.61 \text{ MN/rad.} = \text{Torque/angular displacement}$$

$$= (F_1 \text{ x } r + F_2 \text{ x } r)/\theta$$

and
$$F_1 = k_1 \text{ x } r \text{ x } \theta$$

$$F_2 = k_2 \text{ x } r \text{ x } \theta$$

Therefore
$$0.61 \text{ x } 10^6 = k_1 \text{ x } r^2 + k_2 \text{ x } r^2$$

$$= 1.9 \text{ x } k_2 \text{ x } r^2$$

Therefor $k_2 = 0.61 \times 10^6/(1.9 \times 0.2^2)$

$= 8 \times 10^6$ N/m

and $k_1 = 0.9 \times k_2 = 7.23 \times 10^6$ N/m

For equilibrium, the sum of the horizontal forces must be equal to zero :-

$\therefore$ $F_1 + F_B = F_2$

$\therefore$ $F_B = F_2 - F_1$

$= (8 - 7.23) \times 10^6 \times 0.2$

$= 1.54 \times 10^5$ N per radian of oscillation.

If a torsional stress of ± 25 MN/m^2 is generated in this shaft, scaling the Holzers table (Table 2) indicates that the angular oscillation across the coupling would be 0.6^o which is equivalent to additional compression of the rubber elements by 2.1 mm at a radius of 0.2 m.

Therefore $F_B = 1.54 \times 10^5 \times 0.6/57.3$

$= 1.625$ kN.

This force can be compared to allowable out of balance forces specified in ISO 1940 (5). For a rotor mass of 915 kg and assuming the appropriate balance grade is G6.3 this suggests that the rotor should be balanced to 40 g.mm/kg. This gives a maximum allowable out of balance of $40 \times 915 \times 10^{-6}$ kg.m

$= 0.04$ kg.m

resulting in an out of balance force $= m.r.\omega^2$

$= 0.04 \times (2\pi \times 25)^2$

$= 987$ N

If this was divided equally between both bearings, then the coupling end bearing would be required to withstand an out of balance force of 494 N. The estimated bearing force of 1.625 kN due to torsional resonance is therefore more than 3 times greater than the maximum allowable out of balance force.

Although the exact magnitude of the radial bearing force could not be accurately established it was considered that this proposed mechanism showed the possibility of generating a large, rotating, radial force from a torsional resonant operating condition and could explain the damage that was evident on a number of sets.

8. Remedial Action.

To cure the problem it was necessary to separate the 1st natural frequency of the system from the main torsional excitation frequency to avoid resonance under any load condition. To ensure this, it was necessary to reduce the natural frequency of the system at full load so that it lay below the excitation frequency of 37.5 Hz. This would result in the 1st natural frequency moving further away from 37.5 Hz as the load was reduced. By changing to softer, silicon rubber flexible elements within the coupling it was possible to start with a 1st torsional natural frequency of 34 Hz at full load. This was shown to be far enough away from the excitation frequency to significantly reduce torsional vibration problems. An added advantage of moving to silicon rubber was its ability to operate at higher ambient temperatures.

The bearings and housings of similar sets were inspected and replaced where necessary. Existing and future designs of diesel driven generator sets are to be scrutinised for the possibility of torsional resonance under part load conditions.

9. Conclusions.

The cause of a premature shaft failure on a 634 kW diesel-generator set was traced to an unexpected torsional resonance of the set when operating at part load. The dynamic behaviour was then shown to be the likely cause of excessive bearing housing wear on this and similar sets. Replacement of worn bearing housings and bearings and coupling modifications to reduce the first torsional natural frequency were implemented to resolve the problem.

A review of other sets has been undertaken to ensure the problem does not occur on existing machines. New designs are to be subjected to a more rigorous evaluation of torsional dynamic behaviour.

References:

1 ESDU Data Item 88008 Fatigue Limit of unnotched steels (related to tensile strength. Publ. Engineering Sciences Data Unit, July 1988

2 ESDU Data Item 86028 Fatigue Strength of Keyed Assemblies. Publ. Engineering Sciences Data Unit December 1986.

3 ESDU 81012 Fatigue threshold stress intensity factors and slow crack propagation rates in low and medium strength low alloy steel. Publ. Engineering Sciences Data Unit. Publ. June 1981

4 R.F. Steidel An Introduction to Mechanical Vibrations Publ. John Wiley & Sons, 1980, pp295-305

5 ISO 1940 Balance Quality of Rotating Rigid Bodies Publ. International Standards Organisation 1986.

6 W. Ker Wilson Practical Solution of Torsional Vibration Problems Publ. Chapman & Hall 1948

List of Captions.

Figure 1 View of fractured shaft looking from coupling end towards generator.

Figure 2 View of bearing and housing showing circumferential wear and marking.

Figure 3 Flexible coupling of the type used on the diesel-generator set.

Figure 4 Schematic diagram of diesel-generator system.

Figure 5 Equivalent dynamic model of flexible coupling.

Figure 6 Torsional mode shape for diesel-generator set at full load.

Figure 7 Torsional mode shape for diesel-generator set at 89% load.

Table 1 Holzer table for diesel-generator set at full load.

Table 2 Holzer table for diesel-generator set at 89% load.

Top

Figure 1 View of fractured shaft looking from coupling end towards generator.

I.A. Craighead & T.G.F. Gray

Top

Figure 2 View of bearing and housing showing circumferential wear and marking.

I.A. Craighead & T.G.F. Gray

Figure 3 Flexible coupling of the type used on the diesel-generator set.
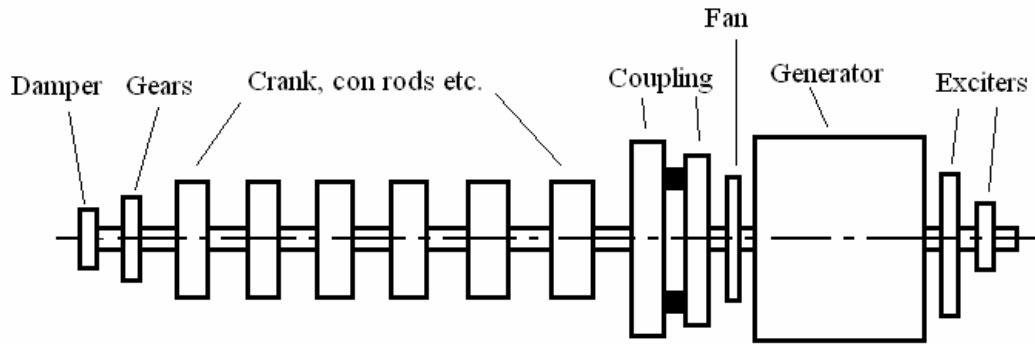
I.A. Craighead & T.G.F. Gray

Top

Figure 4 Schematic diagram of diesel-generator system.

I.A. Craighead & T.G.F. Gray
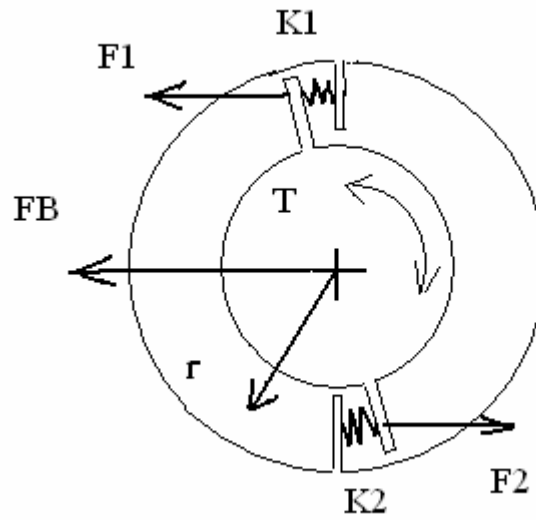
Top

Figure 5 Equivalent dynamic model of flexible coupling.

I.A. Craighead & T.G.F. Gray

Holzer Table for 634 kW Diesel - Generator Set at Full Load

Frequency (Hz) = 40.802 ω^2 =   65723.69

Component	Number	Theta	Inertia (kgm*m)	I*ω*ω*θ	Sum	Stiffness (MNm/rad)	Δθ
Damper	1	1	1.359	89318.49	89318.49	18.76	0.004761
Gear Train	2	0.995239	0.0814	5324.436	94642.92	8.409	0.011255
Cyl 1+7	3	0.983984	0.522	33758.29	128401.2	5.165	0.02486
Cyl 2+8	4	0.959124	0.28	17650.41	146051.6	5.165	0.028277
Cyl 3+9	5	0.930847	0.522	31935.27	177986.9	5.165	0.03446
Cyl 4+10	6	0.896387	0.522	30753.02	208739.9	5.165	0.040414
Cyl 5+11	7	0.855972	0.28	15752.14	224492.1	5.165	0.043464
Cyl 6+12	8	0.812508	0.522	27875.34	252367.4	8.477	0.029771
Flywheel/coupling	9	0.782737	9.528	490162.1	742529.5	0.6101	1.217062
Coupling	10	-0.43432	0.41	-11703.6	730825.9	5.797	0.12607
Fan	11	-0.56039	0.7954	-29295.5	701530.4	13.96	0.050253
Gen rotor	12	-0.61065	16.47	-661007	40523.73	5.066	0.007999
Exciter	13	-0.61865	0.9782	-39773.3	750.3977	1.016	0.000739
P.M. Exciter	14	-0.61938	0.0193	-785.669	-35.2717		

Table 1 Holzer table for diesel-generator set at full load.

I.A. Craighead & T.G.F Gray

Holzer   Table   for   634 kW   Diesel -   Generator Set   at 89%   Load

Frequency (Hz) =   37.5   ω^2 =   55516.43

Component	Number	Theta	Inertia (kgm*m)	I*ω*ω*θ	Sum	Stiffness (MNm/rad)	Δθ
Damper	1	1	1.359	75446.83	75446.83	18.76	0.004022
Gear Train	2	0.995978	0.0814	4500.863	79947.69	8.409	0.009507
Cyl 1+7	3	0.986471	0.522	28587.51	108535.2	5.165	0.021014
Cyl 2+8	4	0.965457	0.28	15007.65	123542.9	5.165	0.023919
Cyl 3+9	5	0.941538	0.522	27285.38	150828.2	5.165	0.029202
Cyl 4+10	6	0.912336	0.522	26439.11	177267.3	5.165	0.034321
Cyl 5+11	7	0.878015	0.28	13648.4	190915.7	5.165	0.036963
Cyl 6+12	8	0.841052	0.522	24373.33	215289.1	8.477	0.025397
Flywheel/coupling	9	0.815655	9.528	431449.3	646738.4	0.501	1.290895
Coupling	10	-0.47524	0.41	-10817.3	635921.1	5.797	0.109698
Fan	11	-0.58494	0.7954	-25829.6	610091.5	13.96	0.043703
Gen Rotor	12	-0.62864	16.47	-574802	35290	5.066	0.006966
Exciter	13	-0.63561	0.9782	-34517.4	772.6028	1.016	0.00076
P.M. Exciter	14	-0.63637	0.0193	-681.847	90.75579		

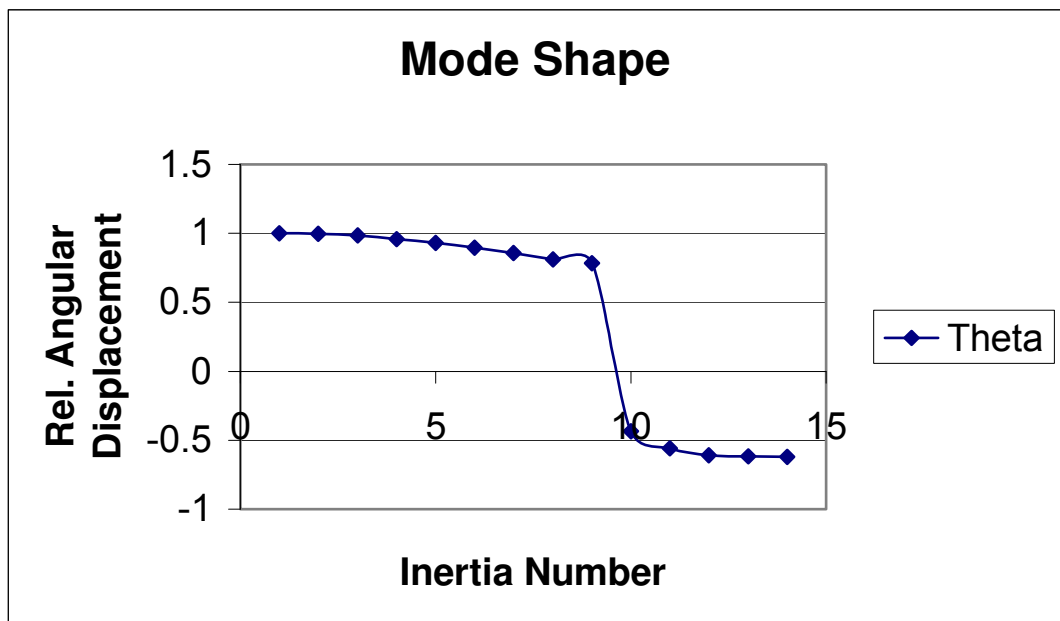Table 2 Holzer table for diesel-generator at 89% Full Load.

I.A. Craighead & T.G.F. Gray

Figure 6 Torsional mode shape for diesel-generator set at full load.
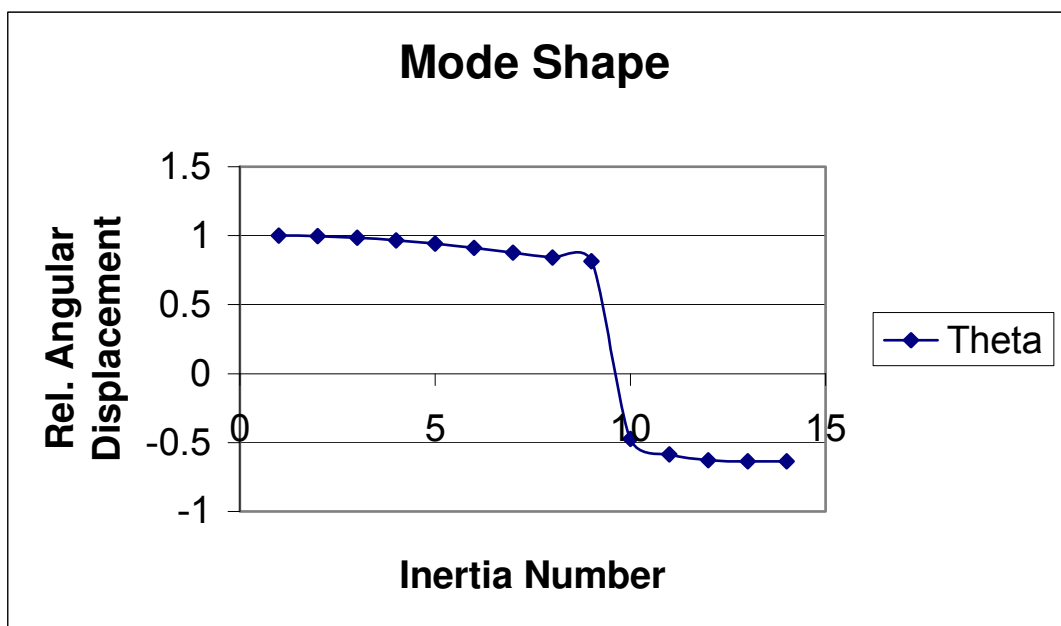
I.A. Craighead & T.G.F. Gray

Figure 7 Torsional mode shape for diesel-generator at 89% load.

I.A. Craighead & T.G.F. Gray